Available online at www.sciencedirect.com
ScienceDirect
Journal of the European Ceramic Society 31 (2011) 2023–2030
www.elsevier.com/locate/jeurceramsoc

Electrical discharge machining of B_4C–TiB_2 composites

Olivier Malek [a,b,*], Jef Vleugels [b], Kim Vanmeensel [b], Shuigen Huang [b], Junhu Liu [c], Sven Van den Berghe [c], Amit Datye [d], Kuang-Hsi Wu [e], Bert Lauwers [a]

[a] K.U. Leuven, Department of Mechanical Engineering, Celestijnenlaan 300B, B-3001 Leuven, Belgium
[b] K.U. Leuven, Department of Metallurgy and Materials Engineering, Kasteelpark Arenberg 44, B-3001 Leuven, Belgium
[c] SCK-CEN, Boeretang 200, B-2400 Mol, Belgium
[d] Department of Materials Science and Engineering, University of Tennessee, Knoxville, TN 37996, USA
[e] Department of Mechanical and Materials Engineering, Florida International University, Miami, FL 33174, USA

Received 4 February 2011; received in revised form 6 April 2011; accepted 17 April 2011
Available online 13 May 2011

Abstract

The interrelationships between the microstructure and electrical discharge machining (EDM) behaviour of B_4C–TiB_2 composites with respectively 30, 40 and 60 vol.% TiB_2 are investigated. Special attention was given to the influence of the grain size on the EDM behaviour by producing composites with an ultrafine TiB_2 phase using in situ synthesis during PECS. The experimental work revealed that 40 vol.% of TiB_2 results in an optimal material removal rate while the surface roughness for rough cut EDM decreases with increasing TiB_2 content. The finer microstructure of the ultrafine composite shows higher MRR's and lower R_a values than the commercial powder based composites. The major material removal mechanism for the PECS based composites was melting. The 3 point bending strength of all composites after grinding, EDM rough cut and EDM finish cut was not statistically different and about 800 MPa. The EDM recast layer was analysed by X-ray photoelectron spectroscopy.

Keywords: Composites; Electrical conductivity; Thermal conductivity; Borides; Electrical discharge machining

1. Introduction

Ceramic materials such as boron carbide, silicon carbide and cubic boron nitride are becoming increasingly popular for wear applications due to their extreme hardness, low specific gravity and stability at high temperatures.[1–3] However, because of their high electrical resistance and hardness, they are particularly difficult to machine using either electrical discharge machining (EDM) or conventional grinding with diamond tooling. Tool stresses, tool wear and the inability to create complex shapes renders diamond grinding less suitable for machining of for example B_4C ceramics. TiB_2 is added to a B_4C matrix to enhance the fracture toughness and strength.[4,5] A fracture toughness of up to 6 MPa $m^{1/2}$ is reported for 40 vol.% TiB_2 ceramics produced by subsequently pressureless sintering at 2175 °C for 2 h and HIP at 2050 °C for 30 min at 200 MPa with free carbon addition, which was co-responsible for the toughening effect.[4,5] B_4C–TiB_2 composites with 20–80 vol.% TiB_2 can also be densified using pulsed electric current sintering (PECS) revealing an increasing fracture toughness and decreasing hardness with increasing TiB_2 content.[6] A fracture toughness of 4 MPa $m^{1/2}$, in combination with a Vickers hardness of 3200 kg/mm^2 and a three point bending strength of 800 MPa are reported for 40 vol.% TiB_2 composites PECS at 2000 °C for 4 min under an applied pressure of 60 MPa.[6]

Besides influencing the mechanical properties, the addition of highly electrically conductive TiB_2 (10.3×10^6 S/m[7]) particles allows increasing the conductivity of the semi-conductor B_4C (2.04×10^2 S/m[7]) matrix, allowing the application of electrical discharge machining (EDM). EDM offers an increased geometrical machining flexibility compared to classical diamond tool grinding.

The goal of this paper is to assess the interrelationships between microstructure, mechanical properties and EDM behaviour of B_4C–TiB_2 composites by investigating the machining behaviour and surface quality of commercially available powder based PECS B_4C composites with 30, 40 and 60 vol.%

* Corresponding author at: Department MTM, Kasteelpark Arenberg 44 – bus 2450, B-3001 Leuven, Belgium. Tel.: +32 16321534.
E-mail address: Olivier.Malek@mtm.kuleuven.be (O. Malek).

0955-2219/$ – see front matter © 2011 Elsevier Ltd. All rights reserved.
doi:10.1016/j.jeurceramsoc.2011.04.024

TiB_2. To assess the influence of the microstructural parameters, an in situ PECS synthesised 30 vol.% TiB_2 composite with substantially finer grain size and a commercially available hot pressed 40 vol.% TiB_2 composite were used as reference materials.

2. Experimental procedure

B_4C–TiB_2 composites were prepared from B_4C (grade HD20, H.C. Starck, $d_{50} = 0.5\,\mu m$) and TiB_2 (grade F, H.C. Starck, $d_{50} = 2.5$–$3.5\,\mu m$) powders. B_4C composites with 30 vol.% in situ synthesised TiB_2 (labelled as 30 vol.% TiB_2 in situ) were made by the reaction of the same B_4C powder, TiO_2 (Grade A-HR, Huntsman Tioxide Europe Ltd., crystal size = 0.17 μm) and carbon black (Grade 4, Degussa, Germany). More information on the in situ PECS synthesis is provided elsewhere.[8] Composite grades with 30, 30 in situ, 40 and 60 vol.% TiB_2, respectively, were prepared by low energy multidirectional mixing (Turbula T2A, WAB, Switzerland) in ethanol for 24 h using ZrO_2 milling balls ($\phi = 5$ mm).

After mixing, the suspension was dried in a rotating evaporator at 65 °C. PECS (Type HP D 25/1, FCT Systeme, Rauenstein, Germany) was performed in a vacuum of 4 Pa. A pulsed electric current was applied with a pulse duration of 10 ms and pause time of 5 ms throughout all the experiments. The powder mixture was poured into a cylindrical graphite die with an inner and outer diameter of 40 and 76 mm, respectively, and sintered for 4 min at 2000 °C, under a maximum pressure of 60 MPa, with a heating and initial cooling rate of 200 °C/min. During PECS, the minimum pressure of 7 MPa was applied during heating and the initial 1 min of the dwell period at 2000 °C and was increased to 60 MPa within 1 min at 2000 °C. The maximum pressure was retained until the completion of an additional 4 min dwell time. The influence of the PECS parameters on the physical and mechanical properties of the B_4C–TiB_2 composites is reported elsewhere.[6] Details on the equipment, die/punch set-up and temperature control are provided in [9]. Hot pressed B_4C with 40 vol.% TiB_2 and 2 wt% free carbon (BT-VR44, ESK Ceramics, Germany) was used as a commercial reference material and labelled as BT 60/40.

The PECS ceramics were ground with a diamond grinding wheel (type D46SW-50-X2, Technodiamant, The Netherlands) on a Jung grinding machine (JF415DS, Jung, Germany) to a constant thickness of 4.5 mm. All EDM experiments were performed on a Wire-EDM machine (Robofil 240cc, Charmilles Technologies S.A.) using a soft brass wire electrode (tensile strength of 500 N/mm^2, $\phi = 250\,\mu m$) and de-ionised water (electrical conductivity of 5 μS/cm). Roughness measurements have been performed on a Form Talysurf-120L (Taylor–Hobson) surface profiler over a length of 8 mm (Cutoff lengths $L_c = 0.8$ mm, $L_s = 0.0025$ mm). The microstructure of the EDM surface was investigated by scanning electron microscopy (SEM, XL30-FEG, FEI, The Netherlands). Phase identification was conducted by a θ–θ X-ray diffractometer (XRD, Seifert, Ahrensburg, Germany) using Cu Kα radiation (40 kV, 40 mA). The flexural strength (sample dimensions 26 mm × 4 mm × 3 mm) was measured on a 3-point bending test set-up (INSTRON 4467, Instron Corp., USA) with a span of 20 mm. A load cell of 5 kN and a loading rate of 0.1 mm/s were used. The reported strength data are the average and standard deviation of 7 bending bars.

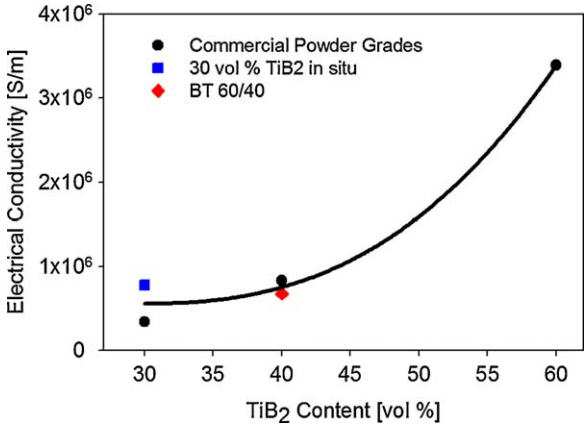

Fig. 1. Electrical conductivity of the B_4C–TiB_2 composites.

The electrical resistance of the samples was measured according to the 4-point contact method using a Resistomat (Model 2302, Burster Präzisionsmesstechnik GmbH, Gernsbach, Germany). Thermal diffusivity and specific heat capacity was measured using a laser flash technique on a Netzsch LFA-457 instrument on 10 mm × 10 mm × 2–4 mm samples in argon with a ramp rate of 100 °C/min from room temperature to 1000 °C. For improved sensitivity at high temperatures, an indium antimonide detector was used. The samples were measured relative to a graphite standard and the data were evaluated using Cowan–Fit non-linear regression software. The thermal diffusivity was measured in the direction parallel to the sintering direction, referred to as the "in-plane" direction.

XPS measurements were performed with an upgraded ESCALAB 220i-XL spectrometer, using monochromatic Al Kα radiation with a typical spot size of about 500 μm. The anode was operated at 15 kV and 150 W. The base pressure is better than 10^{-10} mbar. Depth profiling was carried out by etching the sample surface using a 3 kV Ar^+ ion beam. A current of 1 μA and raster size of 2 mm were used at a chamber pressure of about 8×10^{-8} mbar during etching. At such sputtering conditions, sputtering of a Ag layer with known thickness on a Si wafer resulted in a rate of 3 nm/min. The survey spectra were collected with 100 eV pass energy and 1 eV step size. The high resolution spectra were collected with 20 eV pass energy and 0.05 eV step size. The data acquisition and processing were carried out using the Avantage Data Spectrum Processing Package (Thermo VG Scientific, U.K.).

3. Results

3.1. Electrical and thermal conductivity

The measured room temperature electrical conductivity of the investigated composites is shown in Fig. 1. The formation of a percolating network of TiB_2 particles in a B_4C matrix was established when the TiB_2 content was increased from 20 to 40 vol.%,[6] motivating the minimum amount of 30 vol.% TiB_2

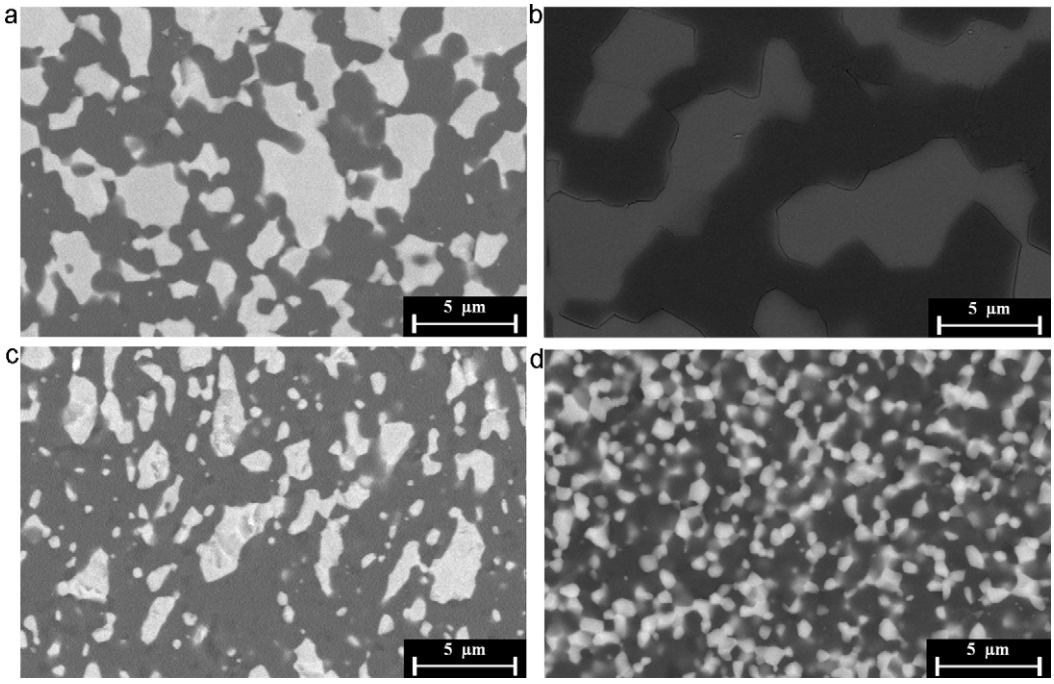

Fig. 2. Backscattered electron micrographs of polished 40 vol.% TiB_2 PECS (a) and commercial BT 60/40 (b) grades and fractured 30 vol.% TiB_2 PECS (c) and TiB_2 in situ (d) grades. B_4C = dark, TiB_2 = bright.

that was used in the present work. Due to this percolating TiB_2 network, the electrical conductivity rises from 6.73×10^3 to 8.12×10^5 S/m when increasing the TiB_2 content from 20 to 30 vol.%,[6] enabling EDM. A similarly drastic electrical resistivity decrease, due to the formation of a percolating network, was also observed for ZrO_2 composites with micrometer sized TiN particle additives.[10]

Assuming an electrical resistivity threshold of 0.3–1 S/m,[11] the composites containing 30 vol.% TiB_2 should be suitable for electrical discharge machining. Backscattered electron micrographs (atomic number contrast) of the 30 and 40 vol.% TiB_2 composites are compared with those of the in situ synthesised (30 vol.% TiB_2) and commercial (40 vol.% TiB_2) ceramics in Fig. 2. The bright TiB_2 phase can be clearly differentiated from the dark B_4C phase, whereas no other phases could be identified within the resolution limit of the SEM. The average TiB_2 particle size, as measured from 200 grains by means of the linear intercept method is 0.95, 1.20, 0.35 and 3.00 µm, respectively.[6]

This TiB_2 particle size difference has a substantial impact on the electrical conductivity, as shown in Fig. 1. The electrical conductivity of the in situ 30 vol.% TiB_2 synthesized PECS grade nearly doubled compared to the commercial powder based composite. Due to the larger grain size of the commercial BT ceramic, containing 40 vol.% TiB_2, compared to the PECS equivalent, the electrical conductivity of the 40 vol.% TiB_2 composite decreased from 8.3×10^5 to 6.7×10^5 S/m.

The thermal conductivity of the ceramics is also of great relevance to the material removal mechanisms. Since melting, evaporation, spalling (thermal shock) and oxidation/chemical reactions are temperature dependent phenomena, the extent of the thermally influenced zone in the material strongly influences the cutting speed, surface quality and MRM. The thermal conductivity of the investigated ceramics is shown as function of temperature in Fig. 3. It should be noted that thermal transport through TiB_2 is mainly performed by electron carriers, due to its high electrical conductivity, whereas it is by means of phonon transport in covalent B_4C.[12] Both materials show a decrease in thermal conductivity with increasing temperature.[12,13] For TiB_2, this is due to the fact that an increased temperature hinders the thermal flow of electrons and consequently lowers the thermal conductivity. In the case of B_4C, an increased temperature increases the phonon density and consequently the increase in phonon umklapp scattering lowers the thermal conductivity.[12] The B_4C starting powder used in this work has a carbon content of 22 wt% and a B/C ratio of 3.7,

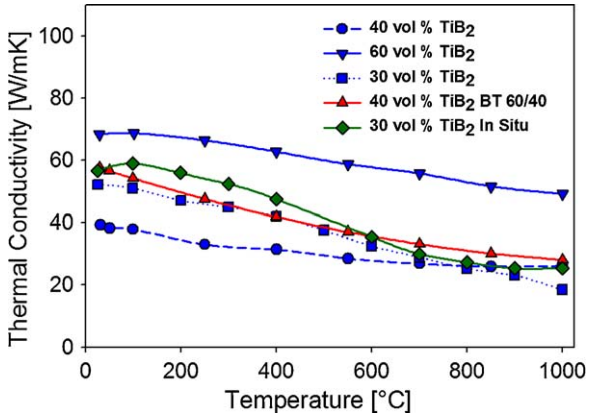

Fig. 3. Thermal conductivity of B_4C–TiB_2 composites.

Table 1
Wire-electrical discharge machining generator settings for the different cutting regimes.

Cut	Regime	Pulse rise time [μs]	Pulse rise time for abnormal pulses [μs]	Pulse interval time [μs]	Generator mode	Open circuit voltage [V]	Offset [mm]
Rough	E501	0.4	0.20	14.0	M 7	80	0.212
	E502	0.1	0.10	6.0	M 37	120	0.163
	E503	0.05	0.05	8.0	M 37	100	0.142
Finish	E504	0.4	0.05	3.0	M 32	120	0.133
	E505	0.4	0.05	0.6	M 30	120	0.130
	E506	0.4	0.05	0.6	M 26	200	0.126

as specified by the supplier. According to Werheit,[14] this super-stoichiometric carbon content results in a considerably higher thermal conductivity compared to stoichiometric B_4C, namely 45 W/mK compared to 15 W/mK.[12]

The thermal conductivity of the 60 vol.% TiB_2 PECS grade is the highest, due to the large quantity of highly conductive TiB_2 (95 W/mK[13]) in the composite. It is expected that the thermal conductivity will decrease with decreasing TiB_2 content. However, the 30 vol.% TiB_2 PECS grade shows a higher thermal conductivity than the 40 vol.% TiB_2 grade.

The reason for this is the amount of grain boundaries in the composite which play an important role in the thermal transport by means of both electrons and phonons. A higher amount of grain boundaries lead to more scattering and consequently a lower thermal conductivity.[15,16] Using values from Huang et al.[6,8] the average overall grain size of the commercial powder based PECS grades can be calculated for 30,40 and 60 vol.% TiB_2 PECS grades to be 1.6, 1.4 and 1.3 μm, respectively. The higher amount of grain boundaries in the 40 vol.% TiB_2 PECS grade, as proven by the lower average grain size compared to the 30 vol.% TiB_2 PECS grade, leads to more phonon and electron scattering and a lower thermal conductivity, see Fig. 3. While the average grain size of the 60 vol.% TiB_2 PECS grade is even lower, the large volumetric quantity of TiB_2 insures high thermal conductivity by means of electron movement.

The larger grain sized hot pressed commercial 40 vol.% TiB_2 BT 60/40 ceramic on the other hand has a significantly higher thermal conductivity than the PECS equivalent. The ranking in thermal conductivity can be completely attributed to a decreasing thermal conductivity with decreasing grain size, i.e. increasing amount of grain boundaries. In addition, highly thermal conductive carbon (119–165 W/mK) present at the grain boundaries or triple pockets[5] enhances the overall thermal conductivity of the commercial BT 60/40 composite. Despite the ultrafine TiB_2 grain size, the PECS 30 vol.% in situ TiB_2 composite also shows a slightly higher thermal conductivity. While the calculated average grain size is very low (0.9 μm[8]), the vastly improved conducting network allows a similar thermal conductivity to be achieved compared to its commercial powder based PECS grade.

3.2. EDM and material removal mechanisms

Wire electrical discharge machining (W-EDM) mainly consists of an initial rough cut, in which the cutting speed is of primary importance, followed by several consecutive low energy finishing cuts to remove the damaged top layer in order to realise a smoother surface with fewer defects. The machine technology settings used in this work are summarised in Table 1. The rough cut is labelled as E501 while the finishing cuts are labelled as E502–E506.

SEM micrographs of the rough cut composites with 60 vol.% of TiB_2 indicate the major MRM to be melting, as shown in Fig. 4a and b. Composites with 30 and 40 vol.% of TiB_2 show a similar behaviour. A resolidified recast layer of 3–4 μm is present on top of the heat affected zone. The rounded edges of the B_4C and TiB_2 grains in contact with the recast layer indicate that this material was molten during the EDM process, which is further supported by the disappearance of clear grain boundaries in the recast layer. Thermal shock damage is clearly visible as sub-surface cracks running along the grain boundaries. The cracks are present in the heat affected zone and are due to the thermal expansion (CTE) mismatch between B_4C ($5 \times 10^{-6}\,^{\circ}C^{-1}$) and TiB_2 ($7.2 \times 10^{-6}\,^{\circ}C^{-1}$) during cooling. The cracks relieve the thermal stresses during cooling, preventing spalling. Fig. 4a and b clearly reveal the absence of spalling, i.e. delamination of the recast layer, and grain fallout due to thermal stresses.

In contrast with the PECS material, which has melting/evaporation as MRM, the main material removal mechanism when EDM in the hot pressed BT 60/40 grade is spalling or thermal shock, as shown in Fig. 4e and f. The reason for this difference is the presence of free carbon in the BT 60/40 ceramic. It was proven by Sigl et al. that the free carbon addition to B_4C–TiB_2 composites is not present as carbon particulates, but as a segregation between the TiB_2 and B_4C grains.[5] This carbon segregation provides an interface which is nearly two orders of magnitude weaker than ordinary grain boundaries. Although this weaker grain interface promotes microcracking and enhances the fracture toughness, it also enhances material removal by spalling off the recast layer together with the outer crystal layer during EDM. The grain interfaces in the thermally influenced surface layer are not strong enough to cope with the thermal expansion differences between the TiB_2 and B_4C grains during quenching, resulting in grain fall out. The EDM surface, shown in Fig. 4e and f, reveals a typical fracture surface appearance instead of a uniform molten recast layer.

The resistance to thermal shock, R, or the maximal thermal gradient a material can withstand can be expressed as a function

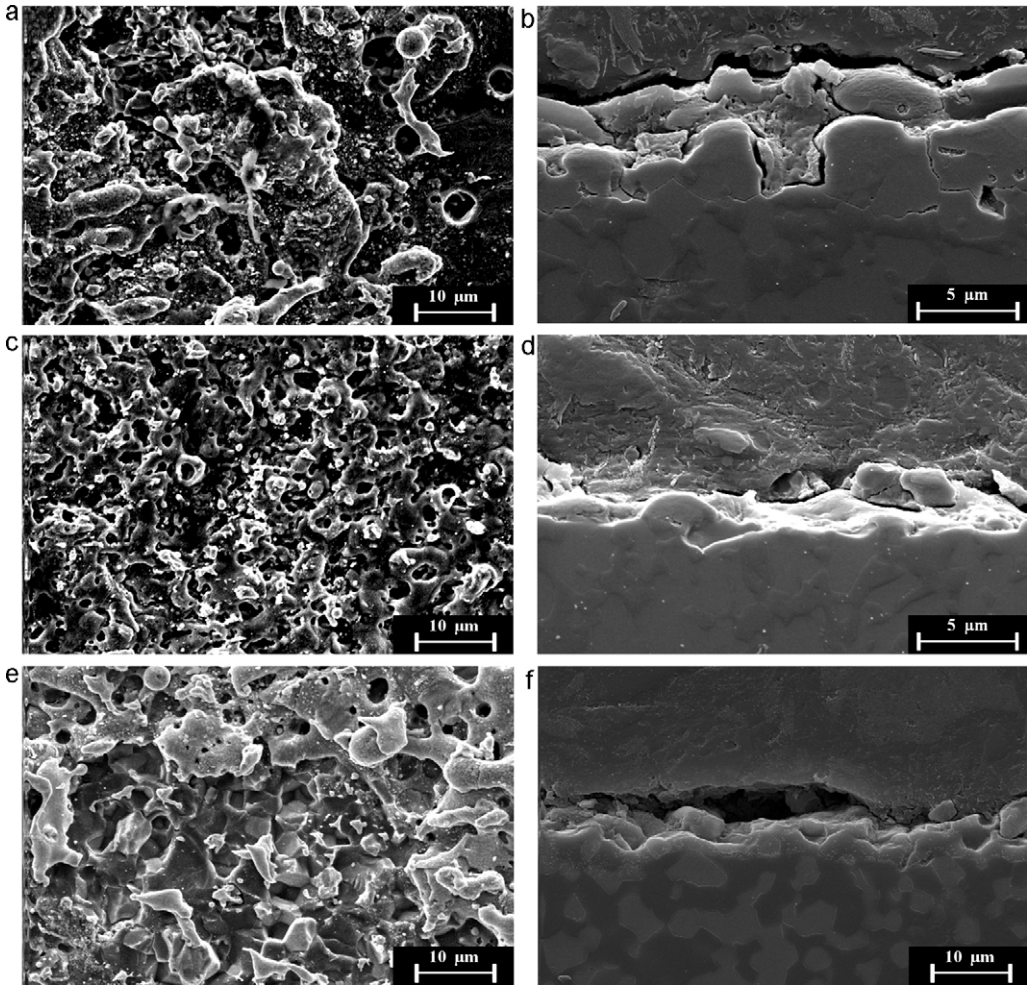

Fig. 4. Surface views and polished cross-sections of rough (E501 regime) (a and b) and finish cut (E506) (c and d) 60 vol.% TiB_2 composites and rough cut (E501) commercial BT 60/40 (e and f).

of the fracture strength, σ_f, Poisson ratio, ν, coefficient of thermal expansion, α, and Young's modulus, E, as[17]:

$$R = \frac{\sigma_f(1-\nu)}{\alpha E} \quad (1)$$

While the Poisson ratio, the thermal expansion coefficient and the Young's modulus of the PECS and BT (60/40) grade can be assumed to be comparable, the strength is not, with only a strength of 400 MPa due to the weaker grain interface in the BT (60/40) composite compared to ~800 MPa for all other grades. This leads to a decreased thermal shock resistance of 50%, which is clearly reflected as a change in MRM.

The recorded MRR's for the E501 rough cut are summarised in Fig. 5, revealing that the MRR increases considerably for the commercial powder based composites when increasing the TiB_2 content from 30 to 40 vol.%. A further increase in TiB_2 content to 60 vol.%, however, lowers the MRR again. Due to the increased thermal conductivity of the 60 vol.% TiB_2 composite, the heat is dissipated deeper into the composite, away from the cutting surface. This is detrimental for the melting/evaporation material removal process, which is primary active in these composite grades, requiring the heat induced by the spark erosion process to be localised. A lower thermal conductivity, such as is the case for the 40 vol.% TiB_2 PECS grade, therefore concentrates the heat at the surface and increases the cutting speed when melting and/or evaporation are the main material removal mechanisms. A direct link between the thermal conductivity and the MRR in the PECS grades based processed from the commercial powders is observed.

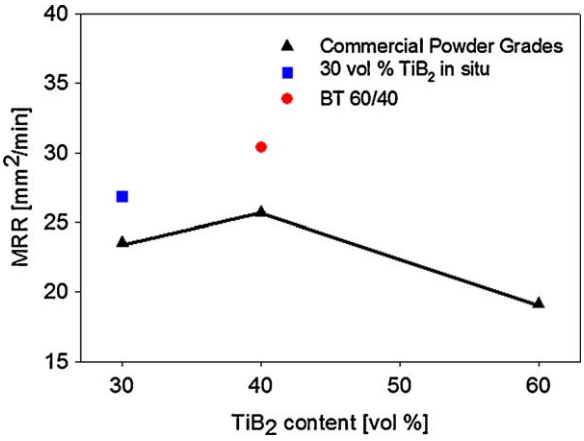

Fig. 5. Rough cut E501 regime material removal rate (MRR).

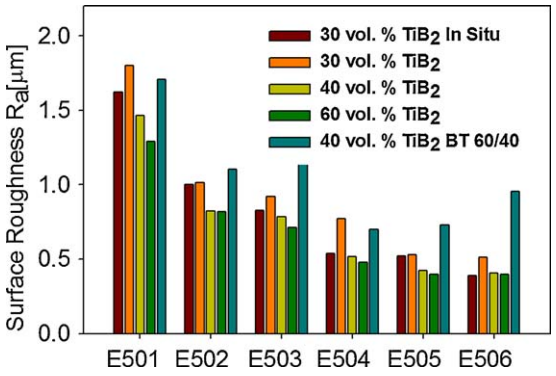

Fig. 6. R_a surface roughness after rough cutting (E501) and finishing passes (E502–E506).

When decreasing the TiB_2 grain size, as for the in situ synthesized 30 vol.% TiB_2 PECS ceramic, the thermal conductivity increases slightly while the electrical conductivity substantially increases (see Figs. 1 and 3). This results in a higher MRR compared to the commercial powder based 30 vol.% TiB_2 equivalent due to the fact that a more stable EDM process is achieved while the melting and evaporation process is only marginally influenced by the small difference in thermal conductivity. At these low electrical conductivities, doubling the electrical conductivity has a profound impact on the MRR, while the electrical conductivity is already sufficiently high enough at TiB_2 contents $\geq$40 vol.% to insure stable EDM.

Because of a different primary MRM, the BT 60/40 ceramic has a much higher MRR than the equivalent PECS grade. While the material initially melts in both grades, the grain interface strength of the BT 60/40 grade is insufficient to cope with the tensile stresses in the heat affected zone generated during cool down after spark erosion. Due to these tensile stresses, spalling occurs allowing to remove more material in a shorter period of time compared to the melting/evaporation MRM.

3.3. Surface quality

The EDM finishing cuts effectively remove the recast layer and part of the heat affected zone, lowering the surface roughness considerably as illustrated in Figs. 4c, d and 6. An increasing electrical conductivity which accompanies an increased TiB_2 content is beneficial for the stability of the EDM process resulting in a lower surface roughness in the E501 rough cut regime (see Fig. 6). This trend is also observed throughout the consecutive finishing regimes.

The higher electrical conductivity of the in situ PECS 30 vol.% TiB_2 grade is translated into a R_a decrease from 1.8 to 1.6 μm when compared to the commercial powder based equivalent. Although the thermal conductivity has a profound impact on the MRR, it does not appear to influence the surface roughness since the MRM of all PECS grades is melting. When progressing towards the finishing cuts, the electrical insulating B_4C grain size becomes a determining factor to the surface roughness. The lower energy levels decrease the depth of the heat-affected zone to the order of the grain size, creating a limit to which the roughness can be decreased. The average grain size of the TiB_2 and B_4C phase is related to the composition.[6] Due to the grain boundary pinning effect of the matrix phase, the size of the secondary phase is limited. At lower TiB_2 contents of 30 vol.%, the B_4C grain size becomes significantly larger than that of the highly conductive TiB_2 phase, ranging from 2 μm B_4C grains at 30 vol.% TiB_2 to 1 μm B_4C grains at 60 vol.% TiB_2 respectively. In the E506 finishing cut, the larger electrical insulating B_4C grains will cause a less stable EDM material removal mechanism and consequently a higher surface roughness. The finishing cut R_a of the 30 vol.% TiB_2 composite was measured to be 0.51 and 0.39 μm for the PECS and in situ PECS grade due to the smaller TiB_2 as well as B_4C grain size in the latter, as shown in Fig. 2.

The surface roughness of the BT 60/40 hot pressed grade is considerably higher in all finishing cuts, as summarised in Fig. 6. This is caused by the difference in MRM, i.e. grain fallout instead of melting/evaporation. The surface roughness that can be obtained is limited by the grain size of the material. This difference in MRM warrants a different EDM technology set. In this case, the last three finishing regimes (E504–E506) introduce more surface defects than they remove. A different EDM technology set with mainly a higher wire offset allowed to achieve a E506 surface roughness R_a of 0.36 μm[18] for the BT 60/40 composite, which is comparable to the roughness obtained for the PECS grades.

In order to assess the composition of the surface layer, X-ray photoelectron spectroscopy (XPS) measurements were performed on polished, E501 and E506 surfaces of the 60 vol.% TiB_2 composite, as summarised in Fig. 7. The Ti 2p spectra of the polished surface before sputtering, shown in Fig. 7a, reveals two peaks associated with TiB_2 at 454.2 and 458 eV.[19]

The Ti 2p spectra of the E501 rough cutting surface, presented in Fig. 7b, show the presence of TiO_2 (459.3 eV) on the top surface. When sputtering deeper into the surface layer, the TiB_2 peaks from the bulk material start to appear. After 20 min of sputtering, only the bulk material composition is detected. The B 1s spectra (Fig. 7c) show a similar behaviour, with a peak of B_2O_3 (197.60 eV) which decreases in intensity and eventually disappears after 20 min of sputtering. The TiB_2 peak in the B 1s spectra (Fig. 7c) slightly increases during sputtering and is maximum when the bulk material is reached. In the C 1s spectra of Fig. 7d, two peaks can be distinguished. Initially before sputtering, only C–C bonds (284.6 eV) are visible. These carbon bonds represent an amount of amorphous carbon in the top layer, introduced by the vacuum system of the XPS measurement setup. After sputtering, a peak related to B_4C (282.8 eV) becomes visible. It is clear that while melting and evaporation are the primary MRM's in the PECS grades, some oxidation takes place as well and the oxides form the recast layer which is visible in the SEM micrographs in Fig. 4. XPS measurements also showed the presence of substantial quantities of brass wire deposits in the form of ZnO and Cu_2O. The Ti 2p spectra of a finished E506 surface resemble the rough cut E501 Ti 2p spectra closely, as shown in Fig. 7e. However, a TiB_2 peak is already visible before sputtering and the oxide peaks decrease more rapidly, indicating a much thinner recast layer.

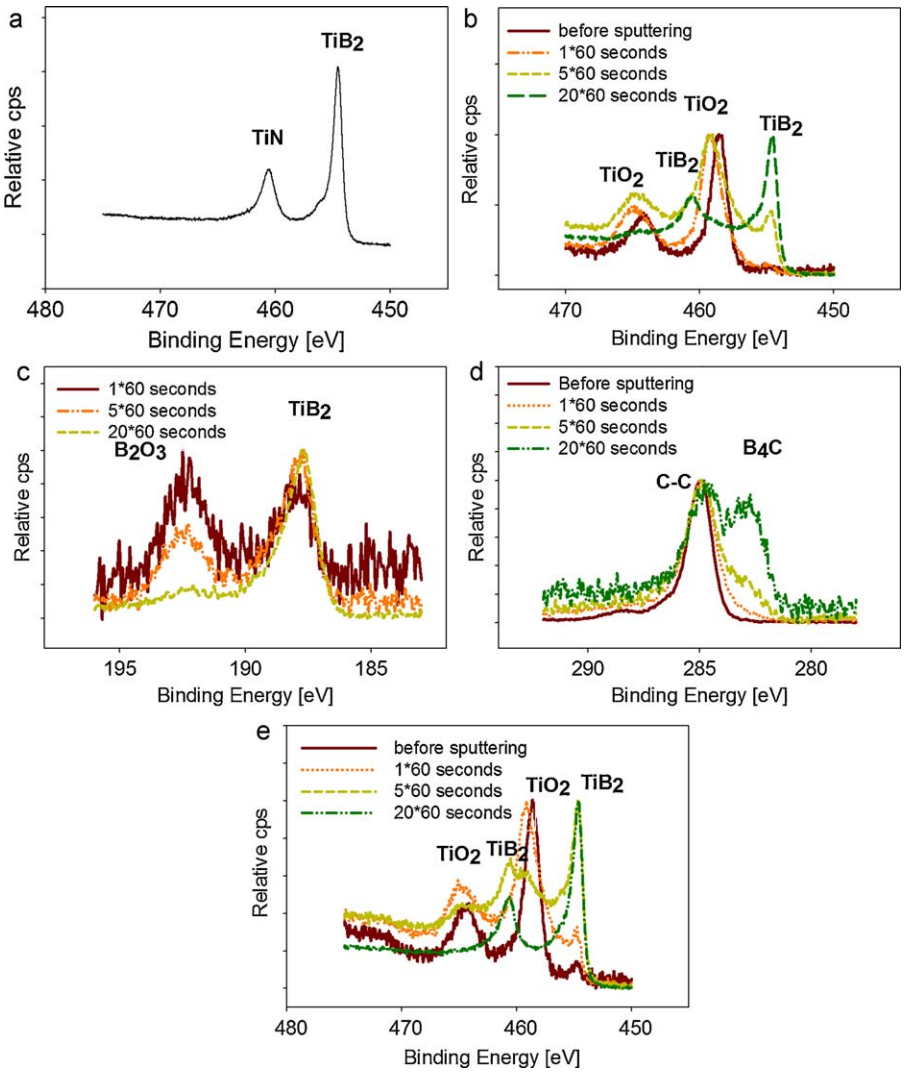

Fig. 7. Ti 2p XPS spectra of a polished (a), E501 rough cut (b) and E506 finishing cut (e) surface of a 60 vol.% TiB_2 composite, together with the B 1s (c) and C 1s (d) spectra of the E501 rough cut surface.

3.4. Surface defects and stresses

The most appropriate way to assess the influence of the surface quality of high strength ceramics is flexural strength testing. Three types of surface conditions were investigated, namely ground, rough cut E501 and after the E506 finishing cut. All measurements have been performed within 24 h after EDM machining or grinding. The flexural strengths are presented in Fig. 8. With increasing TiB_2 content, the strength slightly rises from 742 ± 139 MPa at 30 vol.% TiB_2 to 867 ± 131 MPa for the 60 vol.% TiB_2 PECS grade with a ground surface. The decreased grain size after in situ synthesis increased the as-ground strength from 742 ± 139 MPa to 865 ± 58 MPa for the 30 vol.% TiB_2 grades. The 40 vol.% TiB_2 commercial hot pressed grade has a substantially lower ground strength of 441 ± 42 MPa, due to the weaker B_4C–TiB_2 grain interface and the larger grain size.

When considering the surface quality, rough cutting EDM lowers the strength of all composite compositions with ~100 MPa. However, keeping the standard deviations of 100–150 MPa in mind, it can be concluded that the decrease

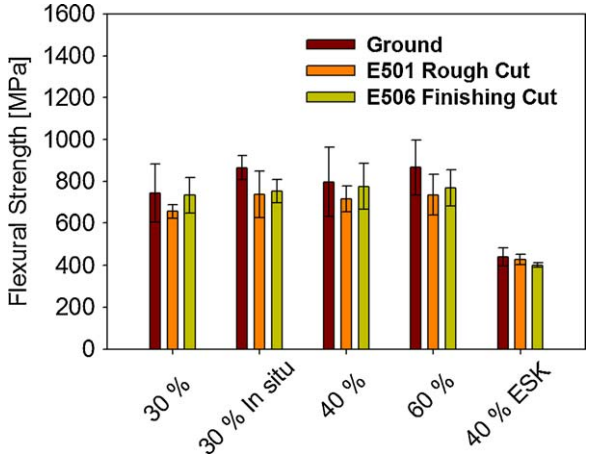

Fig. 8. Flexural strength as function of TiB_2 content and surface finish.

is not statistically significant. When decreasing the amount of defects on the surface, such as microcracks and surface roughness, due to the application of finishing cuts, the average strength rises slightly again to almost the strength of the as-ground ceramics. However, it has to be noted, that this also happens within the standard deviation width. Due to the low interface strength and MRM by spalling, the 40 vol.% TiB_2 commercial hot pressed grade does not show any deterioration after rough cut EDM or improvement after finishing EDM, indicating that the surface roughness is not the critical flaw size determining factor in this material. In the hot pressed material, the weak grain interface determines the flexural strength, which is independent of the surface quality. XRD measurements of the EDM E501, E506, ground and polished surfaces indicate no peak shifts, implying that no residual (tensile) stresses are introduced by EDM which are detrimental to the flexural strength. Moreover, grinding does not introduce compressive residual stresses neither.

4. Conclusions

The electrical and thermal conductivity of B_4C–TiB_2 composites are strongly related to the volume percentage of TiB_2 in the composite. A higher TiB_2 content leads to an increased electrical conductivity, while the thermal conductivity of the composite is also influenced by the average grain size in the composite. Grain refinement due to in situ synthesis greatly increases electrical conductivity, whereas the thermal conductivity was only slightly influenced by the creation of a suitable electron conductive path through the composite.

SEM investigation revealed the main material removal mechanisms in the PECS composite grades to be melting and evaporation. When increasing TiB_2 content from 30 to 40 vol.% in the PECS grades, the decrease in thermal conductivity increased the material removal rate and the increased electrical conductivity lowered the rough cut surface roughness due to an increased EDM stability. At 60 vol.% TiB_2, the increased thermal conductivity results in a better heat dissipation into the composite, leading to a lower MRR. The increased electrical conductivity however further decreased the surface roughness.

The addition of carbon, as in the commercial hot pressed 40 vol.% TiB_2 composite, lowers the grain interface strength and overall composite strength, changing the MRM to grain fallout/spalling/thermal shock. The reduced thermal shock resistance increased both the MRR and surface roughness.

XPS investigation of the surface layer of the PECS composites revealed the recast layer to be composed of amorphous TiO_2 and B_2O_3. The finishing EDM cuts effectively lower the thickness of the surface layer.

Due to the negligible strength reduction after EDM compared to grinding, B_4C–TiB_2 composites prepared by means of PECS are suitable for applications in which EDM is the machining method of choice.

Acknowledgements

This work was financially supported by the Fund for Scientific Research Flanders (FWO) under Project No. G.0539.08. This work was supported by the Commission of the European Communities within the FP6 framework under Project No. STRP 505541-1, in which ESK Ceramics supplied the commercial boride composite. K. Vanmeensel thanks the Fund for Scientific Research Flanders (FWO) for his post-doctoral fellowship. The authors thank AgieCharmilles for their support with the EDM equipment.

References

1. Riley F. *Structural ceramics: fundamentals and case studies*. Cambridge University Press; 2009. ISBN 978-0-521-84586-1.
2. Thevenot F. Boron carbide – a comprehensive review. *J Eur Ceram Soc* 1990;**6**:205–25.
3. Schwetz KA, Sigl LS, Greim J. Wear of boron carbide ceramics by abrasive waterjets. *Wear* 1995;**181–183**:348–55.
4. Sigl LS, Schwetz KA. Fracture Resistance of B_4C–TiB_2 composites. *Jpn J Appl Phys* 1994;**10**:224–5.
5. Sigl LS, Kleebe H-J. Microcracking in B_4C–TiB_2 composites. *J Am Ceram Soc* 1995;**78**:2374–80.
6. Huang SG, Vanmeensel K, Malek OJA, Van der Biest O, Vleugels J. Microstructure and mechanical properties of pulsed electric current sintered B_4C–TiB_2 composites. *Mater Sci Eng A* 2011;**528**:1302–9.
7. Berger LI. *Semiconductor materials*. CRC Press Inc.; 1997. ISBN 0-8493-8912-7.
8. Huang SG, Vanmeensel K, Van der Biest O, Vleugels J. In situ synthesis and densification of submicrometer-grained B_4C–TiB_2 composites by pulsed electric current sintering. *J Eur Ceram Soc* 2011;**31**:637–44.
9. Vanmeensel K, Laptev A, Hennicke J, Vleugels J, Van der Biest O. Modelling of the temperature distribution during field assisted sintering. *Acta Mater* 2005;**53**:4379–88.
10. Salehi SA, Van der Biest O, Vleugels J. Electrically conductive ZrO_2–TiN composites. *J Eur Ceram Soc* 2006;**26**:3173–9.
11. Konig W, Dauw DF, Levy G, Panten U. EDM-future steps towards the machining of ceramics. *Ann CIRP* 1988;**37**:623–31.
12. Nishi Y, Arita Y, Matsui T, Nagasaki T. Isotope effect on the thermal conductivity of Boron Carbide. *J Nucl Sci Technol* 2002;**39**:391–4.
13. Munro RG. Material properties of titanium diboride. *J Res Natl Inst Stand Technol* 2000;**105**:709–20.
14. Werheit H. Boron-rich solids: a chance for high-efficiency high-temperature thermoelectric energy conversion. *Mater Sci Eng B* 1995;**29**:228–32.
15. Cremers CJ, Fine HA. *Thermal conductivity*. Springer; 1990. ISBN 978-0-306-43672-7.
16. Yang H, Bai GR, Thompson LJ, Eastman JA. Interfacial thermal resistance in nanocrystalline yttria-stabilized zirconia. *Acta Mater* 2002;**50**:2309–17.
17. Goldsmid HJ. Thermal shock resistance of electrical insulators. *Brit J Appl Phys* 1963;**14**:463–4.
18. Brans K. Electrical discharge machining of advanced ceramics. PhD Thesis, K.U. Leuven; 2010, ISBN 978-94-6018-178-8.
19. Lu F-H, Chen H-Y. XPS analyses of TiN films on Cu substrates after annealing in the controlled atmosphere. *Thin Solid Films* 1999;**355–356**:374–9.